A Virtual Reality and haptic simulator for ultrasound-guided needle insertion

Ma Alamilla, Charles Barnouin, Richard Moreau, Florence Zara, Fabrice Jaillet, Tanneguy Redarce, Fabienne Coury

A Virtual Reality and haptic simulator for ultrasound-guided needle insertion

Ma. Angeles Alamilla, Charles Barnouin, Richard Moreau, Florence Zara, Fabrice Jaillet, Tanneguy Redarce and Fabienne Coury

***Abstract*—Articular and soft tissue punctions or injections are widely used for the diagnosis and the treatment of rheumatic disorders. Ultrasound is increasingly used to guide these interventions in order to correctly position the needle in the target area, and thereby improve the efficiency and safety of the procedure. During their learning, medical students need to practice in order to master the manipulation of the needle and the ultrasound probe at the same time and acquire enough skills before practicing in a real patient. To offer a risk-free training for apprentices, we present in this paper the design and development of a simulator based on Haptics and Virtual Reality. We described in particular two main aspects of our prototype: (i) the model of forces involved in the needle insertion and their haptic rendering; (ii) the 2D ultrasound image rendering of the virtual environment. Their combination provides the student with a realistic experience. An additional 3D view is also presented, that serves as pedagogical tool useful in the learning process. Experimental validation and preliminary evaluation by the medical partner show that our prototype exhibits sufficient stability and realism for a good immersion in the training scene.**

***Index Terms*—Virtual Reality, training medical simulator, needle insertion, haptics, ultrasound rendering.**

I. Introduction

MEDICAL students need to practice several times to master and perfect the clinical procedures they will confront. These processes require students to be in capacity to correctly dose the force exerted onto the patient's tissue, to avoid injuring or damaging him/her while performing the gesture. Thus, to provide practical training, cadavers or manikins can be used. This option allows medical students to feel quite similar haptic sensations as if interacting with a real patient. However, using cadavers presents some limitations, as for instance getting an authorization from the relatives, and ethics approval [1]. Also the tissue remains permanently deformed after the first use, and the physical properties are changing as the body decays, like blood irrigation or tissue stiffness. In the case of manikins, they are available only for some specific medical procedure training. Moreover, although they can be used several times, they wear down and become disposables over time. Moreover, their haptic feedback remains questionable.

Ma. Angeles Alamilla, Richard Moreau and Tanneguy Redarce are with Univ Lyon, INSA Lyon, Université Claude Bernard Lyon 1, Ecole Centrale de Lyon, CNRS, Ampère, UMR5005, 69621 Villeurbanne, France.

Charles Barnouin, Florence Zara and Fabrice Jaillet are with Univ Lyon, UCBL, CNRS, INSA Lyon, LIRIS, UMR5205, F-69622 Villeurbanne, France.

Fabienne Coury is with Department of Rheumatology, Hopital universitaire Lyon Sud, Hospices Civils de Lyon, Université Lyon 1.

Virtual Reality (VR) based simulators are quite common as they offer objective feedback and different case scenarios [2]. However, they often lack realistic haptic feedback which is key in improving medical skills of the trainee [3].

In this context, the use of VR with haptic devices has been an increasing option in recent years. The idea is to create a new generation of medical training simulators. They combine a numerical simulation (reproducing the organs behavior) and a haptic device (reproducing the kinesthesic sensation) in order to perceive the consequences of the medical gesture. Moreover, they allow working in different environments with force feedback to help them to immerse in diverse situations [4], [5]. The use of these new simulators also reduces the time spent on patients enabling to complete the training faster, and allowing to extrapolate their acquired skills to a real-life situation. Finally, these VR and haptic simulators offer to medical students a way to improve and gain skills before practicing on real patients [6], [7], [8], [9].

In [10], authors provide a recent state-of-the-art in needle insertion training based on haptic interaction. They conclude that simulators coupling VR and haptic feedback are the most promising one, and also that developing realistic simulators is quite challenging. In this paper, we focus on the development carried out to provide a simulator that could be used as a new way to learn ultrasound guided needle insertion. The development of the two parts of such simulators still remains a strenuous task. Indeed, the different inherent stiffness of the body parts such as skin, fat, muscles, tendons, or bones has to be realistically reproduced. One example of such complexity appears in the development of a simulator for ultrasound-guided articular needle insertion. This gesture is considered to be a challenging medical gesture as it not only requires a good knowledge of anatomy, but it also requires bimanual coordination of an ultrasound probe and a needle at the same time to ensure correctly the progression of the needle through the articulation to the target area.

In this paper, we present a medical training simulator for needle insertion that offers full immersion and realism as close as possible to the real procedure. This simulator is divided into two main parts: (i) a mechanical part composed of two haptic devices in order to reproduce the involved forces during the needle insertion; (ii) a Virtual Reality part that generates a 2D simulated ultrasound image, in order to propose the usual view available during this medical gesture. This view enables the user to visualize the needle position and the tissue deformation in the virtual environment. Let note that several mathematical models (obtained from the literature, plus an original one) are

used to compute the involved forces during gesture. Moreover, the proposed prototype has been designed in collaboration with our medical partners to place the students in a immersive and comfortable position.

The aim of this paper is to validate the main features of the simulator. The paper is structured as follows. In section II, the needle insertion procedure and the forces involved during gesture are introduced. In section III, the general view of our simulator is presented. It consists of a mechanical and a Virtual Reality part coupled together. In section IV, the algorithms to render the different forces involved in the needle insertion process are described. In section V, the process to render an ultrasound view of the 3D scene is detailed. In section VI, preliminary results are presented, to validate the rendering of the force and its realism. Finally, section VII concludes this paper and introduces future work.

II. About puncturing and its training

A common procedure in rheumatology consists in performing infiltration or puncture into joints to reduce pain [11]. This procedure is commonly accomplished using ultrasound images. Thus, the physician uses an ultrasound probe in order to monitor the needle tip during its progression [12]. Let note that manipulation of both needle and probe is quite challenging and require the development of a motor-visual coordination and dexterity. This dexterity is mainly acquired by practicing and companionship under expert supervision.

A. Involved forces during puncturing

This subsection is dedicated to the presentation of the forces involved during the puncture procedure. Fig. 1 illustrates the three stages that can be distinguished during puncture [13] whereas the needle pierces soft tissue. Each of these stages generates a set of forces that need to be rendered through the haptic device.

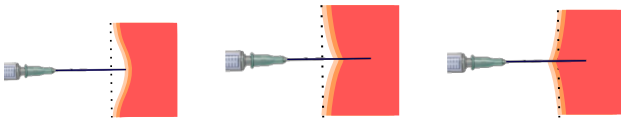

(a) Pre-puncture (b) Puncture (c) Withdrawal

Fig. 1: Three stages can be distinguished during the needle insertion in soft tissue: pre-puncture, puncture, withdrawal.

a) Pre-puncture: A force appears when the needle is pushing the surface of the tissue which becomes distorted without being pierced. Several authors have parameterized the tissue behavior in this case. One model is proposed in [14] where they describe it as a visco-elastic interaction. We denoted this force as $\vec{f}_{\text{pre-puncture}}$.

b) Puncture: Once the needle pierced the skin, several forces are involved to reproduce the action of cutting soft tissues. Three kind of forces [15] are contributing during the puncture due to the needle shaft rubbing against the tissue whereas it cuts the tissue. These forces (viewed in Fig. 2) are:

- **Cutting force** ($\vec{f}_{\text{cutting}}$) which acts on the needle tip in the axial direction. Its intensity depends on the penetrated tissue and the needle tip shape.
- **Friction force** ($\vec{f}_{\text{friction}}$) which tends to be in the opposite direction of the motion. This force is due to the surrounding tissue.
- **Clamping force** ($\vec{f}_{\text{clamping}}$) which acts on the side of the needle shaft in the normal direction by the tissue that surrounds it and constrain the needle's movements.

c) Withdrawal: The last stage occurs when the needle is withdrawn. The body offers an axial force ($\vec{f}_{\text{withdrawal}}$) similar to the cutting force but in the opposite direction.

d) Hard contact: We can also consider the **hard contact force** ($\vec{f}_{\text{hardContact}}$) which only occurs when the needle collides with a rigid object such as a bone for instance. This force is high enough to give the sensation that the needle is touching an impenetrable surface.

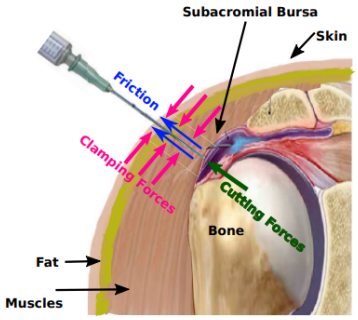

Fig. 2: Interaction forces during needle insertion.

At the end, considering that *(soft)* refers when the needle is inside of soft tissue and *(hard)* when the needle collides with a bone, the total force involving during needle insertion is:

$$\vec{f}_{\text{total}} = \begin{cases} \vec{f}_{\text{pre-puncture}} + \vec{f}_{\text{friction}} \\ +\vec{f}_{\text{cutting}} + \vec{f}_{\text{clamping}} & \text{(soft)} \\ +\vec{f}_{\text{withdrawal}} \\ \vec{f}_{\text{hardContact}} & \text{(hard)} \end{cases} \quad (1)$$

B. Previous work about needle insertion simulators

Kurita et al. [16] instrumented a Geomagic Touch in a virtual environment. A virtual needle can interact on a rubber sheet to obtain several forces like the pushing force from the needle and the reaction force of the rubber sheet. Despite introducing the rubber to improve the rendering forces, it does not allow it to work with different layers at the same time, with different tissues, nor hard surfaces like the bone.

Forest et al. [17] propose the use of two identical haptic devices to achieve a simulator for ultrasound-guided needle puncture: one haptic device is used to render the needle forces during the insertion, and the other to simulate the ultrasound probe. They created a virtual environment in which a 2D image ultrasound is displayed during the performance. This image is based on data obtained from real ultrasound images. Only one anatomy is thus available on this simulator which limits its application as a learning tool. Another drawback comes from the fact that the simulator does not offer hand support where the user can lie his hand to avoid trembling during the needle insertion which limits the realism of the simulated procedure.

Magee [18] introduces another ultrasound-guided needle simulator using a mannequin to represent the patient. The

ultrasound probe and the needle are instrumented with 3D position sensors. On a screen, a software recreates the ultrasound image. Concerning the force feedback, the needle has a slide mechanism that contracts itself when collisions occur with the plastic mannequin. This simulator allows puncturing any part of the patient's body but does not constrain the needle's movements, allowing thus to move the needle in any directions inside the body which is unrealistic as the tissues always limit the needle's displacement.

In [19], authors describe an augmented reality simulator for femoral palpation and needle insertion. For the palpation part, they used two *Novint Falcons* devices that support the touching zone which recreates the behavior of the patient's skin. To simulate the needle insertion, they modified the end effector of *Phantom Omni* so it looks like a real needle. The force feedback is taken from a set of recorded data of multiple patients. Although the presented results are satisfactory for the palpation part, the needle insertion simulations lack realism as the *Phantom Omni* does not offer angular restraint during the needle insertion, allowing to rotate it in any direction.

In [20], a VR simulator for anesthesia training is presented. This simulator uses pre-recorded data to determine the patient's tissue behavior during the insertion, and a *Phantom Omni* with VR glasses to provide immersion to the student. Although this system allows the student to choose any entry point, it does not provide any wrist restriction, nor any limitations on the needle's orientation.

In [21], authors present a haptic and VR simulator for liver biopsy. This work present the different components but it remains unclear how they coupled them. Moreover, it does not take into account the tissue deformation on US images and the needle orientation on the haptic interface.

In conclusion, several main characteristics are missing in existing needle insertion simulators which limit their realism:

- the needle's advancement is not restrained which induces a non realistic insertion;
- the involved forces are not correctly rendered;
- the forces are not differentiated whereas that must be rendered to represent each inner layer of the tissue;
- no hand support is proposed, where physicians can lay on their hands over as in real procedures;
- no ultrasound image suitable for any anatomy or pathological case is proposed;
- no feedback on tissue deformation are provided, whereas that is considered as essential by practitioners to track the needle in the ultrasound view.

III. Our contributions

To improve the existing needle insertion simulators for puncture gesture training, we propose a complete simulator based on haptics and VR technologies. Thus, several components have been developed and gathered to provide this immersive environment.

- We proposed a "mechanical part" based on two haptic devices representing the ultrasound probe and the needle. This mechanical part includes also a hand support representing the patient's skin.
- We implemented several rendering forces to supply with the tactile feeling and the haptic feedback during the needle insertion.
- We developed a VR part to visualize the virtual scene (anatomy, needle, probe) in 3D and in 2D.
- We proposed a real time US view of the 3D scene. It is computed according to the location/orientation of the US probe and needle. It enables the visualization of the needle and resulting tissue deformations during the manipulation of haptic devices (*i.e.* during the puncturing).
- We offered an easy to set and flexible solution for shoulder joint, that can be easily adapted to large joints (knee, hip). No need for fastidious medical image preprocessing to integrate new 3D scenes and exercises.

A. Mechanical part of the simulator

Fig. 3 presents the mechanical part of our simulator including two haptic devices. A Virtuose™ 6D Desktop (Haption SA, Soulgé-sur-Ouette, France) (see right picture) is used for the needle. Its 6 degrees of freedom can be controlled in order to reproduce forces up to 10 N. It lies on a base which includes a hand support that represents the patient's skin. The user can thus lie his hand on it during the needle insertion, gaining comfort and stability during the gesture. One tip of the rod, which represents the needle, is attached to the haptic device. On the other tip, a mock syringe is attached. To ensure realism, this mock syringe was built matching the dimensions of a real one. An insertion point has been set in the hand support to allow the rod to freely pass through. Moreover, the stylus of a Geomagic® Touch™ (3D Sytems, Los Angeles, USA) (see left picture) is used to represent the ultrasound probe. It can be freely moved around the insertion point as in real procedure.

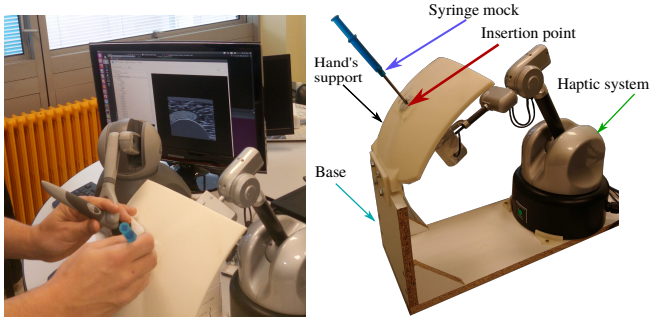

Fig. 3: Mechanical part of the simulator with a focus (right picture) on the haptic device used for the needle including a mock syringe mock and a hand's support.

B. Virtual Reality part of the simulator

Fig. 4 presents two significant views provided by the VR part of our simulator: (a) a pedagogical textured 3D view of the complete scene with transparency; (b) a 2D ultrasound view similar to the one provided by the probe.

The first one enables to show global interactions in the scene. It permits to infer internal location of the tissues and needle, with their relative displacements. This choice is based on what is called didactic transposition, a process that aims to create the optimal conditions for learning, relying on the real conditions for the gesture but also paying attention to

the processes of construction of knowledge [22]. The second one proposes an ultrasound view to guide the gesture as in the medical room. This 2D view is generated according to the probe and needle position/orientation. Thus, a complete pipeline is proposed to obtain a real time US view integrating the deformations involved by the needle insertion.

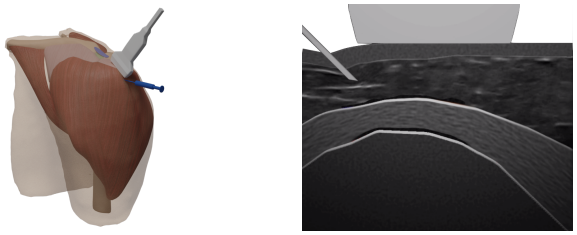

(a) 3D pedagogical view (b) 2D US view with deformation

Fig. 4: Two views proposed by the Virtual Reality part.

C. Interactions between mechanical and Virtual Reality parts

To propose an ultrasound view according to the position/orientation of probe and needle, which are both manipulated by the user thanks to two haptic devices, the mechanical part of the simulator is coupled to the VR part to transmit adequate information, in both ways. Thanks to this combination (illustrated in Fig. 5), the user can practice the needle insertion under echography and develop the motor-visual coordination required to manipulate both tools, needle and ultrasound probe.

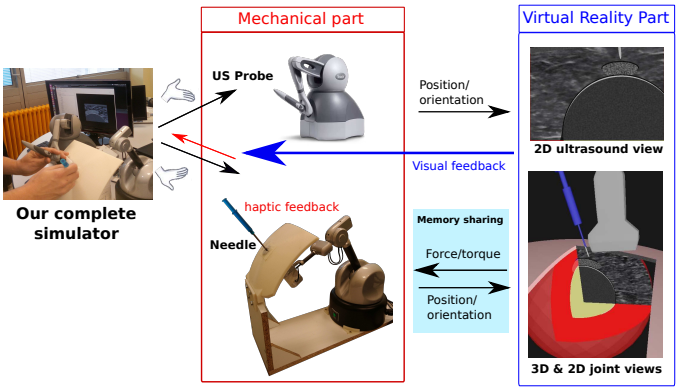

Fig. 5: Coupling between the mechanical and VR parts.

For this coupling, we created a virtual shared-memory using *Boost* [1]. It allows the haptic environment to share the position and orientation of the tools (needle and probe) with the virtual reality environment. This latter uses the needle location to identify the different layers of tissue that are being punctured, as well the force exerted by the virtual limb (see next section for the force computation details). The probe location will serve to generate the cutting plane where the 2D image will be constructed, with various ultrasound effects, integrating as well the deformation due to the tools interaction on the tissues.

[1]The boost C++ libraries https://www.boost.org/

IV. Rendering forces on the haptic interface

The main objective of the haptic interface is to properly render all the involved forces during the needle's insertion, in order to provide an adequate feedback to the user during this medical gesture. A survey of force models is proposed in [23].

A. Pre-puncture

For the pre-puncturing force, we use the model obtained in [24], where the authors parameterized it by inserting a needle in a bovine liver. As the pre-puncture behavior is non-linear, the model is based on a second-order polynomial, where the force increases steadily, and a sharp drop occurs when the skin is finally pierced. It is defined by:

$$\vec{f}_{\text{pre-puncture}} = \begin{cases} 0, & P_{tip} < d_1 \\ a_1 P_{tip} + a_2 P_{tip}^2, & d_1 < P_{tip} \leq d_2 \\ 0, & P_{tip} > d_2 \end{cases} \quad (2)$$

where P_{tip} is the needle tip position, d_1 is the starting position of the layer, d_2 is the end position of the layer. The values of a_1 and a_2 are obtained by the authors to fit a real puncture, with $a_1 = 0.0480$ N/mm and $a_2 = 0.0052$ N/mm^2.

B. Puncture and withdrawal

Cutting and withdrawal. To reproduce the cutting force, the "tracking wall" method is used [25]. It is based on a virtual spring to compute the cutting forces. This approach is used with classic algorithms like the *God-object* which is focused on giving the user the sensation of exploring a surface [26]. The difference with classic methods is that no damper is required to dissipate the energy. It is substituted by a second wall which tracks the tool position during the displacement to help keeping the force constant. The method gives the possibility to set the virtual limb in any part of our workspace [25]. Let's notice that this method enables to provide for the puncture: (i) different tissue stiffness; (ii) the ability to perform stops inside the virtual joint; (iii) the small rejection force generated by the muscles when the needle stops. The force obtained by this method is:

$$\vec{f}_{cutting} = K_t(\Delta_h)\vec{e} \quad (3)$$

where K_t is a tuning parameter representing the stiffness of the penetrated tissue, Δ_h is the distance between the current needle tip position and the position of the "tracking wall", $\vec{e}$ is the director vector of the trajectory. The same method is used for the withdrawal force, but in the opposite direction.

There is no real consensus in the literature for living tissue [27], but we can extract an approximate value of K_t. It is then refined with the help of a medical expert in order to reproduce a behavior similar to reality.

Let's note that some other approaches have been proposed to render the cutting and withdrawal forces. They are based on bio-mechanical models or finite element methods. However, despite their accuracy, these methods are well known for being very high computation consuming and not be able to work with real-time simulations [28]. Thus, our original method overcomes these problems, and both solves chattering and allows to perform stops inside the tissue in real-time.

Friction. For the friction force, instead of using a general approach as the Coulomb model, we opted for a more realistic one designed especially for needle insertion. In [29], the authors used the LuGre model which is a dynamic model based on the microscopic representation of irregular contact surfaces and elastic bristles. The LuGre model uses an internal state z that represents the bending of the bristles. It is given by:

$$\dot{z} = v - \frac{\sigma_0 |v|}{g(v)} z, \tag{4}$$

where v is the velocity of the insertion, σ_0 is the stiffness coefficient for the microscopic deformations during pre-sliding displacement, $g(v)$ describes the Stribeck effect. This last effect is given by:

$$g(v) = \mu_c + (\mu_s - \mu_c) e^{-\beta |v|}, \tag{5}$$

where μ_c and μ_s are the Coulomb and friction coefficients, and β is a constant determined by parametrization. So, the friction force computed by the LuGre model is determined as:

$$\vec{f}_{\text{friction}} = \vec{F}_n (\sigma_0 z + \sigma_1 \dot{z} + \sigma_2 v), \tag{6}$$

where σ_1 is the damping coefficient associated with $\dot{z}$, σ_2 is the viscous damping and $\vec{F}_n$ is the injection cutting force.

The model parameters have been experimentally obtained by making a periodic penetration in a *Gellan Gum (E418)* with a needle attached to a 5-DoF manipulator [29]. Based on this work, table I presents the parameter values used.

Parameter	σ_0	σ_1	σ_2	μ_c	μ_s	β
Value	2.592	0.879	2.04×10^{-3}	1.763	0.052	0.075

TABLE I: LuGre model's parameters used in our simulator.

Clamping. To implement the clamping force, we opted to use a virtual fixture [30] which corresponds to sensory information that overlays the environment feedback. This sensory information is used to establish limits or virtual borders, in order to restrain the user movements. In our simulator, we use the approach described in [25], wherein the virtual fixture provides a bilateral restriction that ensures the needle to move along the desired path. The desired trajectory is defined once the user starts its gesture. He estimates the correct trajectory according to the images provided by its US probe. Once its needle is inside the body, he will feel the clamping forces when it deviates from this initial trajectory. Thus, the haptic device exerts an orthogonal force in order to reproduce the tissue resistance.

Moreover, as one of our objectives is to allow the medical student to choose the initial inclination of his/her entry point on the virtual joint, it is thus not possible to establish a predefined trajectory for every case. So the trajectory of the needle and the clamping forces need to be calculated once the user has initiated his gesture inside the patient joint. To overcome this point, the tool orientation is obtained using quaternions provided by the haptic device.

For this, when the tool pierces the tissue, the current quaternion is stored as q_0, which will be our reference to follow the orientation. So if the user changes the tool orientation, it will be necessary to calculate the deviation between the stored quaternion and the current one q_c to exert the correction forces to correct. For that, the quaternion rotation is computed using the following equation describing the rotation from q_0 to q_c:

$$q_r = q_c^{-1} q_0 = (q_{r0}, q_{r1} i, q_{r2} j, q_{r3} k). \tag{7}$$

The term q_{r0} refers to the real component, and the remaining three terms are the imaginary components.

Once this is done, the rotation corresponding to the angle of the relative rotation is calculated using:

$$\theta_{qr} = 2 \cdot \arctan(q_{\text{rnorm}}, |q_{r0}|), \tag{8}$$

where the euclidean norm q_{rnorm} is calculated by:

$$q_{\text{rnorm}} = \sqrt{q_{r1}^2 + q_{r2}^2 + q_{r3}^2}. \tag{9}$$

Thus, the orientation error is obtained by:

$$\vec{\varepsilon}_{qr} = \{q_{r1}, q_{r2}, q_{r3}\}^T * \frac{\theta_{qr}}{q_{\text{rnorm}}}. \tag{10}$$

Moreover, the trajectory generator is established by:

$$\vec{\tau}_{qr} = k\, \vec{\varepsilon}_{qr} - B\vec{v}, \tag{11}$$

where k and B are parameters describing the nature of the tissue; $\vec{v}$ is the tool velocity. As for the cutting forces, k and B values are predefined based on literature and their final values are obtained empirically based on expert's experience.

It is thus possible to compute the difference of orientation compared to the initial trajectory. A simple proportional control law is then applied to determine the magnitude of the clamping force to apply.

Hard contact.

As haptic interface stiffness is limited, hard contact can not be reproduced correctly. To solve this issue, Kuchenbecker et *al.* [31], proposed a method based on decaying sinusoid. It describes the dynamics of contact with rigid objects as two superimposed forces: a high-frequency one, and another with a slower extended response. The defined force response is computed depending on the time lapse and the incoming velocity of the tool, with:

$$\vec{f}_{\text{hardContact}} = A\ |v_{in}|\, e^{\ln(0.01) t/d} \sin(2\pi f t), \tag{12}$$

for $0 < t < d$, where A is the nominal amplitude ($A = 19.9$ Ns/m), d is the fixed duration ($d = 0.055$ s), and f is the frequency ($f = 55$ Hz). They measured acceleration while tapping on wood with a needle tip, and they identified the parameters A, d, and f in order to have similar responses. We then experimentally adjusted the amplitude A with the user's feeling. The benefit of this method is that the system remains passive thanks to the fact that the force is only computed during a short lapse of time.

V. Virtual Reality part with US rendering

The aim of our complete VR haptic simulator is to propose exercises for the training of needle insertion gesture. Fig. 7 shows an example of the 3D view performed by the VR part. It represents a virtual joint used during the exercises as well as the corresponding ultrasound rendering. Thanks to this VR

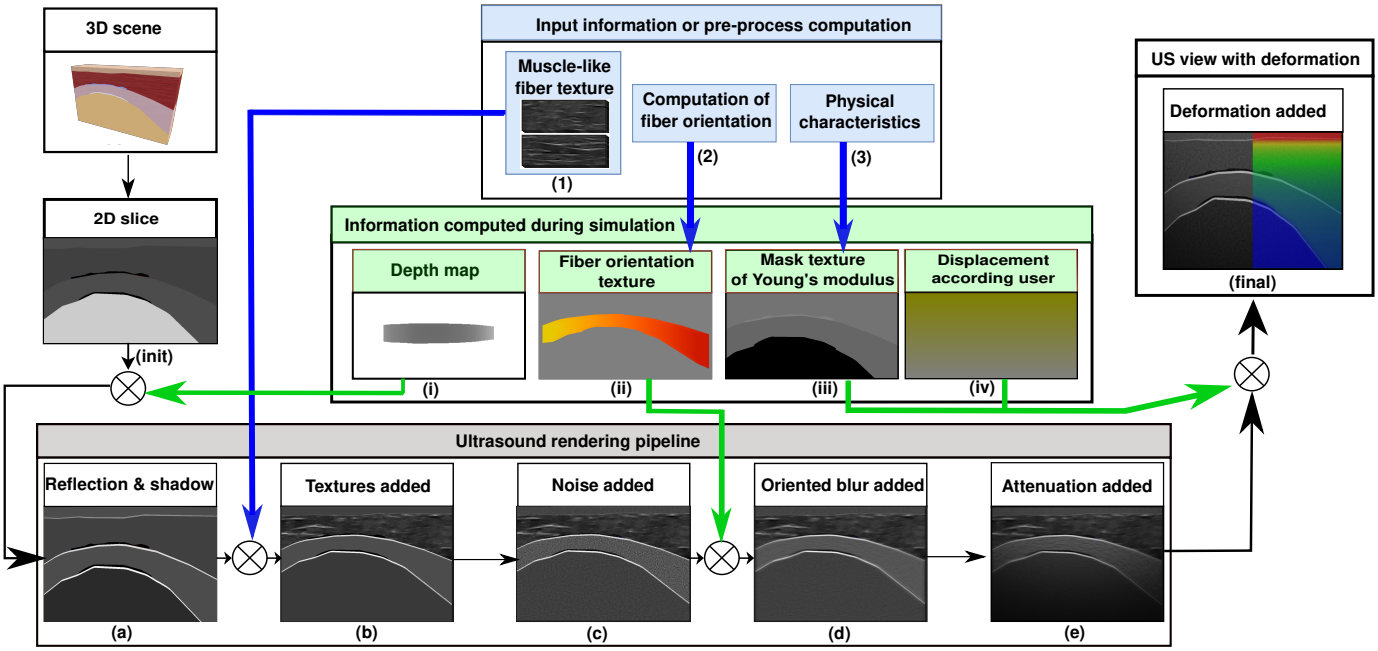

Fig. 6: Rendering pipeline to provide the ultrasound view which is deformed according to the needle insertion.

part, the user can explore the joint using the ultrasound probe mock, identify the tissues and choose a path line to the target. During this exploration, the user is also able to rotate freely the virtual 3D scene. Once the insertion point is chosen, the user can insert the needle in the tissues with the desired orientation. Moreover, while the needle is inserted, the user can move its ultrasound probe and visualize the needle progression in a offset 2D ultrasound image generated in real-time.

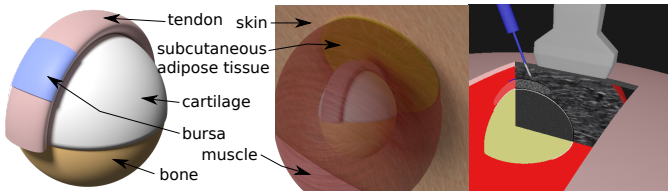

Fig. 7: 3D scene and view provided by the VR part.

Fig. 8 presents the different modules of our framework for the VR part. It has been developed in C++/OpenGL. We used an Intel® Core™ i7-6800K CPU, an NVIDIA® GeForce® 1070GTX and 31.3 GB of memory for the following results.

The collision detection between haptic devices and objects in the 3D scene is treated in a same thread for both needle and probe, as long as the needle does not pierce the first layer of the object. Moreover, the used algorithm considers the direction and velocity of the needle to obtain accurate collision points [32] and correctly treat the puncturing.

We now focus on our complete rendering pipeline (illustrated by Fig. 6) which permits to generate the ultrasound view (see (e)) which is then deformed (see (final)) according to the manipulation of the haptic devices. This process enables a realistic ultrasound view for the simulator.

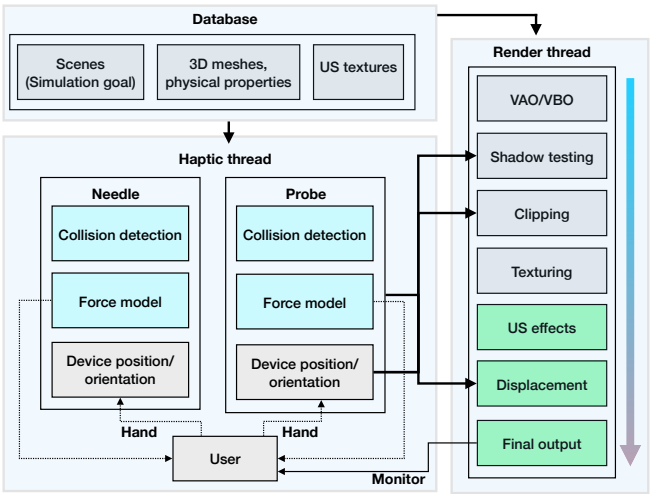

Fig. 8: Our framework developed for the VR part.

A. *Ultrasound rendering pipeline on a 2D slice*

The first step of the rendering process consists in computing a 2D slice (see (init)) of the 3D scene by using the *Capping Clipped Solids* method [33] according to the probe position.

Then, we apply the method proposed by [32] to successively add on this 2D slice all the effects required to provide an ultrasound view. Thus, the reflection and shadow are both added (see (a)) by filling a depth map, computed during the simulation (see (i)), into the texture before any other render pass. To add attenuation effect, the speckle is approximated by a *Perlin* noise (see (c)) and the shadow rendering pass is used to add absorption effect. Note that for thick tissue, we directly apply a texture (see (b)) acquired by selecting a zone with a representative pattern of the tissue from a reference image (see (1)). For this, we both consider the lateral and longitudinal orientations, with the result illustrated on Fig. 9.

Fiber orientation of thin tissues. To consider the orientation of thin tissues, some others treatments are performed providing a texture-dependent oriented blur [32]. Firstly, a pre-computed process consists in retrieving the fibers orientation (see (2)). It is computed for all vertices thanks to the specific geometry of tendon-like tissue. The direction is set by the smallest principal curvatures via quadratic fitting [34]. Secondly, the oriented blur (Fig. 10) works in two steps during the generation of the US view. The considered 3D tissue is clipped in the ultrasound plane according to the probe position, and its surface is colored according to the orientation of the fibers (see (ii)). This image is then used as an input to post-process the noisy image to create the oriented blur (see (d)). Then, the blurred picture is mixed with the image obtained with the reflection and shadow effects to create the final ultrasound picture (see (e)) of the rendering pass.

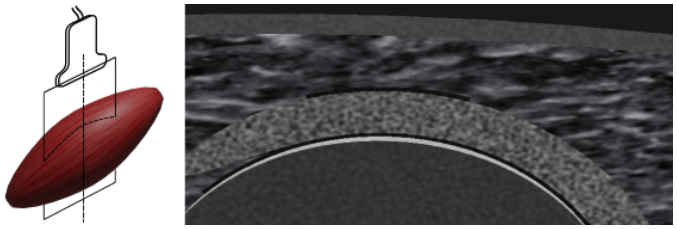

(a) Longitudinal view

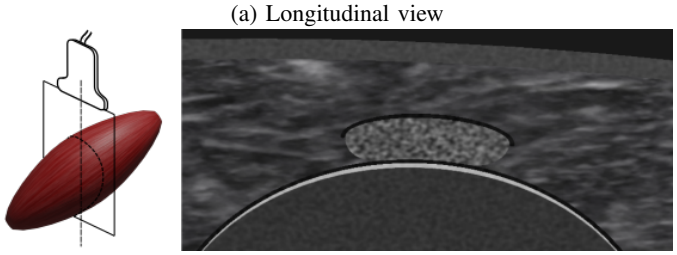

(b) Transversal view

Fig. 9: Fiber texture according to probe orientation.

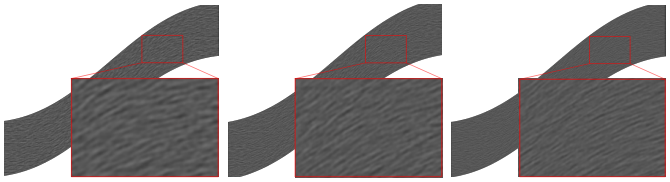

(a) Large fibers (b) Medium fibers (c) Thin fibers

Fig. 10: Different grain-size noises for several fibers display of thin tissues.

B. Deformation of the ultrasound view

To take into account the interaction of the two haptic devices, we apply their displacements (see (iv)) directly into the pixels of the computed ultrasound picture (see (e)) [32].

For the displacement due to the needle insertion, the idea was to fit the results obtained by Gao et *al.* [35] to simulate the deformation of the skin, and those obtained by Crouch et *al.* [36] to simulate the inner tissues deformation involved after puncture. Thus, the displacement due to the needle, before puncture, is defined by:

$$d(\tilde{r},z,E) = \begin{cases} z_{max}\, g\left(2-\frac{\tilde{r}}{R_{max}}\right),\ z < z_{max} \\ \frac{\|\vec{f}_{\text{pre-puncture}}\|}{E}\, g\left(\frac{\tilde{r}}{R_{max}}\right),\ z > z_{max} \\ 0,\ \tilde{r} > R_{max} \end{cases} \tag{13}$$

where $g(t) = 1-(3t^2-2t^3)$, $\vec{f}_{\text{pre-puncture}}$ is the pre-puncture force as defined in subsection II-A, E is the Young modulus of the tissue at the point $(\tilde{r},z)$.

Fig. 11 illustrates that R_{max} is the influence radius of the needle from Crouch's model (with $R_{max} = 2cm$), $\tilde{r}$ is the cylindrical coordinate r, when $z < z_{max}$ (point A), $\tilde{r}$ is the spherical coordinate r when $z > z_{max}$ (point B). Indeed, as the needle pushes the surface, the displacement of the tissue at the needle tip is exactly equal to the displacement of this same tip.

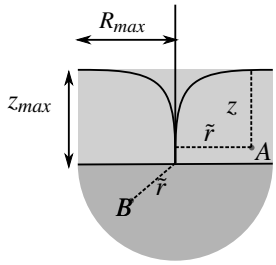

Fig. 11: Two zones of effect for the displacement function: along (light gray) / beneath (dark gray) the needle tip.

And after puncture, the friction and cutting forces affect the tissues along the shaft and also below the needle. Locally, the friction force is dominant along the shaft, while the cutting force is dominant under the tip. It means that we can also split our displacement function in two, as follows:

$$d(\tilde{r},z,E) = \begin{cases} \frac{\|\vec{f}_{friction}\|}{z_{max}\,E}\, g\left(2-\frac{\tilde{r}}{R_{max}}\right),\ z < z_{max} \\ \frac{\|\vec{f}_{cutting}\|}{E} g\left(\frac{\tilde{r}}{R_{max}}\right),\ z > z_{max} \\ 0,\ \tilde{r} > R_{max} \end{cases} \tag{14}$$

where $\vec{f}_{friction}$ and $\vec{f}_{cutting}$ are the same forces defined in subsection II-A. Let's remark that $\vec{f}_{friction}$ is divided by z_{max} as the friction force is spread along the needle.

These displacements depend on the Young modulus of the tissues in order to improve the realism. Fig. 12 shows some results obtained for the displacement of the soft tissues due to the needle, considering a single, or two values of E for the tissues ($E = 0.5$ and 5 N/mm^2 for top and bottom layers). Fig. 13 gives an example of displacement map taking into account the needle orientation, and the resulting US image.

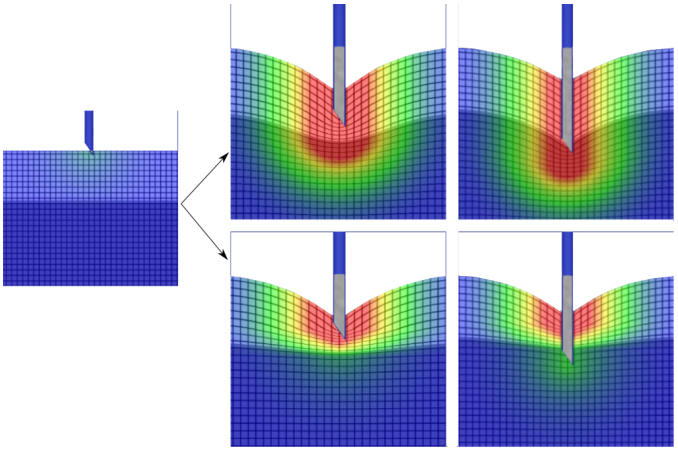

Fig. 12: Deformation due to the needle considering a single (top row) or two values of E (bottom row) for tissues.

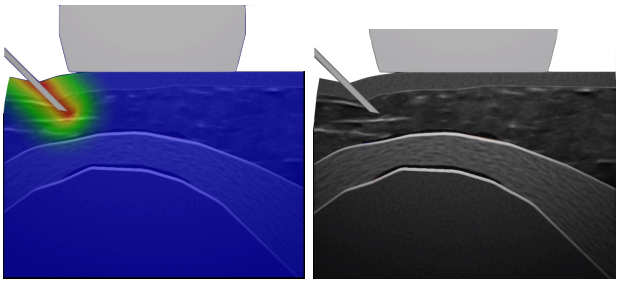

Fig. 13: Deformation due to the needle inserted at a 45° angle.

C. Performance

We performed several tests to analyze the performance. Even for $7,864,320$ triangles, our rendering pipeline runs in about 0.002s including deformation and all the effects in the US image, which is enough for real-time.

VI. Experimental validation

The aim of this paper is to propose a first validation of the features available on our simulator. Thus in this section, we will present some experiments to validate our needle insertion simulator. Experiments have been conducted in order to validate separately the different components of the simulator.

It is important to firstly validate the needle force feedback. We thus proposed to our medical expert different tests in order to check the realism of the force feedback while puncturing. The different parameters can also be adjusted according to expert feedback. The cutting and the clamping forces were tested in basic situations to check their realism according to the expert experience. More experiments could then be processed including a full face and content validity with a larger population involving novices and experts.

In this context, the first subsection demonstrates the main problem while using commercial haptic interface to reproduce soft contact: the chattering phenomenon. Our proposed method solves this issue and allows us to reproduce different cutting forces. The second subsection is dedicated to the validation of all the forces involved during puncturing. Users can feel the forces in 3D as it happens in real procedures.

A. Validation of the cutting/withdrawal forces

Commercial haptic devices are built for quick implementation. Thus to generate force, it is only necessary to apply the desired one using the communication protocol or API given by the manufacturer. This approach is called *Direct Method*. It does not include any mathematical model to compute the required force. But, as we will demonstrate in this section, some problems occur with these rendering haptic methods.

Firstly, Fig. 14 shows a test made with a Haption Virtuose™ 6D desktop. On this figure, the wall (which can represent the surface of the skin) is depicted with the blue line and the tool with the green line. The virtual wall is set with a reaction force of 1 N. The tool can be freely moved while it is above the wall. Then, the user moved it until it collides with the virtual wall at $t \approx 4$ s. When the force is applied to the haptic device, this produces an effect called *chattering*. It is represented by the high-frequency change of force and speed. The chattering effect is a phenomenon that occurs when a sudden change of force happens in the haptic device. Moreover, this effect disturbs the force feedback sensation and can damage the haptic device if the force or frequency is high enough. The same phenomenon happens at $t \approx 7.5$ s when the user stops exerting effort on the tool, the haptic device tends to reject the tool outside of the wall, as there is no more opposing force from the user. This behavior does not correspond to the desired one, showing that the direct method can not be applied on our system.

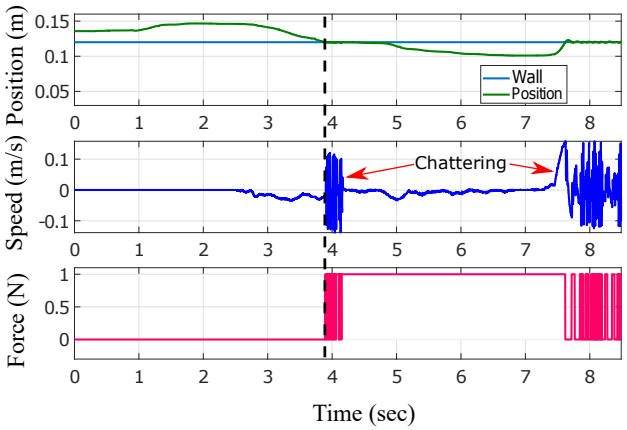

Fig. 14: Force injection performed with direct method.

To avoid chattering, our solution consists to use the tracking wall method to model the environment. More details are available in [25]. Fig. 15 shows the results obtained with a spring environment with a stiffness of 250 N/m. As it can be observed, when the haptic device tool collides with the wall at $t \approx 3.5$ s, the chattering effect is attenuated, as the force increases smoothly according to the advancement of the user. However, as soon as the user stops inside the wall ($t \approx 13$ s), the system rejects the tool, forcing it to exit from the wall and giving the sensation of deformation of the tissue. The needle behavior is thus realistic according to our medical expert: this method allows us to properly reproduce the force feedback while a tissue is cut.

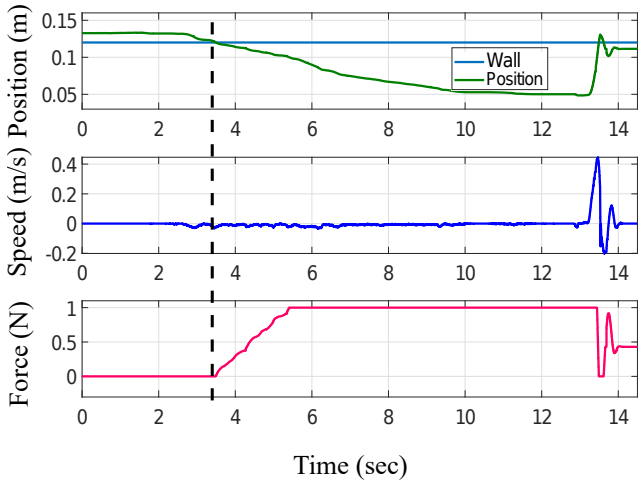

Fig. 15: Spring environment model.

B. Validation of the complete simulated puncture

Secondly, we consider the forces involved during the insertion of the needle inside a shoulder (which corresponds to the exercise scene of Fig. 7). While puncturing, the user should both: (i) feel forces while going through the different shoulder's layers; (ii) handle the US probe on a deported ultrasound rendering in order to watch the needle inside the tissues. Concerning the haptic feedback, the values of the cutting forces used were based on the expertise of our medical partner and the characterization obtained during the needle insertion in a bovine liver [27]. A value is thus defined for each layer (skin, muscle, bursa, tendon, cartilage, bone) of the shoulder of our experimental setup. But, it can be easily modified to offer different training scenarios. The values used in this work are gathered in Table II.

Tissue	Skin	Muscle	Bursa	Tendon	Cartilage	Bone
Force (in N)	1	2	1.5	2.5	3	4

TABLE II: Setup values used during the "shoulder" exercises.

In this context, we performed two exercises to get feedback from a medical expert of the the needle's trajectories and forces involved during puncture. In these tests, we mainly focus on the needle insertion but user has access to the US rendering if necessary. The first exercise consisted of inserting the needle following, as much as possible, a straight line without deviating from the initial trajectory. The goal of this exercise is to let the user feel the different layers while puncturing. For the second one, the objective is to test the forces while changing the trajectory. This may happen when the user detects a wrong direction (thanks to its US probe) and wants to change its trajectory. So an expert was asked to insert the needle with an incorrect trajectory and then change the needle's trajectory.

Trajectories Fig. 16 and Fig. 17 show the trajectories that the user performed during both tests. Fig. 18 shows the displacement in the Cartesian space for both insertions. As mentioned previously: the first insertion was performed in a straight line without any change in the trajectory; during the second one, the user performs a change of trajectory inside the virtual limb. The blue lines represent the user trajectory and the (purple or red) small arrows the clamping forces. We observe the expected behaviors in both tests.

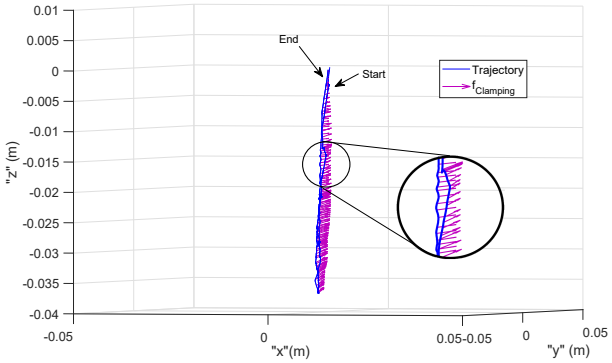

Fig. 16: Needle insertion without changing direction.

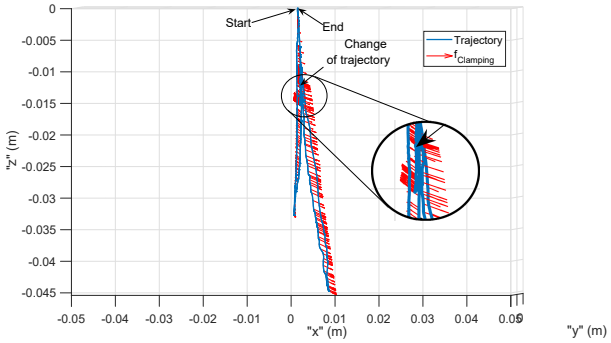

Fig. 17: Needle insertion with changing direction.

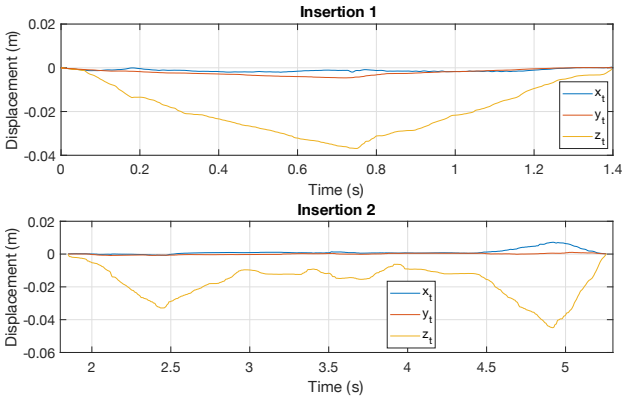

Fig. 18: Needle displacement for both tests.

Forces. The clamping forces were computed when the user unintentionally or intentionally departs from the desired trajectory, *i.e.* when the tip of the needle deviates from the initial direction. Indeed, these forces are due to the tissue reaction when it is compressed during insertion. Fig. 19 presents these forces for both tests. In the first one, the user was not able to totally remain in the desired trajectory despite the instructions which explains the presence of clamping forces. In the second insertion, it is seen how the clamping forces are computed when the user changes the trajectory. The force increases

because of the trajectory modification but when the user starts advancing, these forces decrease since a new trajectory is chosen. However, as the user is in the final part of the insertion and his withdrawal does not follow the trajectory, the clamping forces are greater to simulate the forces exerted by the surrounding tissue.

Fig. 20 shows the cutting forces rendered for both tests. On these plots, it is seen how the cutting force (*i.e.* $f > 0$) is generated while the user pierces the virtual limb, and how the withdrawal force (*i.e.* $f < 0$) is generated when the needle is withdrawn from it. For the first insertion, the user pierces with constant motion until $t \approx 0.7$ s, and then he withdraws the needle. For the second insertion, the user pierces with constant motion until $t \approx 2.5$ s, after that he withdraws the needle, and at $t \approx 3$ s he tries to find the correct needle's orientation. During this part, the user tries to keep the same depth while orienting correctly the needle but, due to its unintentional movements, a small variation of cutting and withdrawal forces are generated. At $t \approx 4.4$ s, he inserts again his needle with the new orientation, the cutting force increases until a certain depth at $t \approx 4.9$ s. After touching the bone, he finally decides to withdraw entirely the needle.

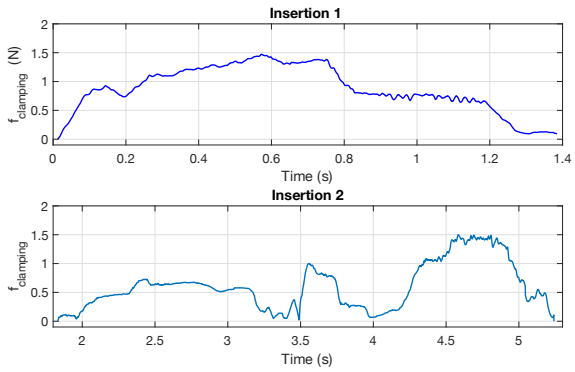

Fig. 19: Clamping forces according time for both tests.

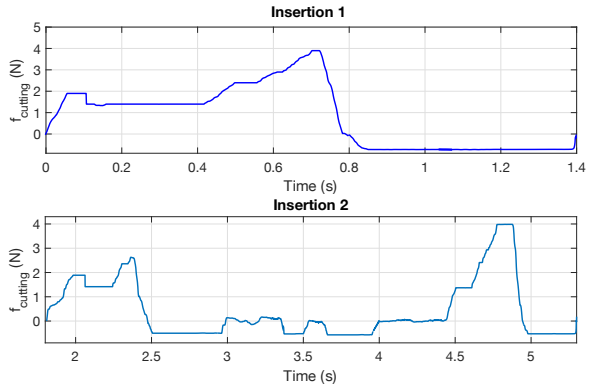

Fig. 20: Cutting forces according time, for both tests.

These exercises allow us to test different cases and to check if the haptic feedback satisfies an expert. According to our medical partners, the haptic rendering is sufficiently realistic to reproduce a first training in order to gain experience. All the reproduced forces in this work allow them to immerse themselves in the simulation.

VII. Conclusion and Future Work

We have presented in this paper, a complete simulator for ultrasound-guided needle insertion. The main objective is to assist the user in gaining motor and visual coordination, skills that are quite difficult to acquire but are mandatory to perform needle injections or puncture at reduced risks for the patient. This simulator is composed of two parts: a mechanical component including a haptic interface that provides a tactile sensation during gesture; and a Virtual Reality part with a remote ultrasound 2D rendering used to guide the medical gesture. This Virtual Reality part also enables a 3D view of tissues and instruments, both probe and needle, as a pedagogical view (that is not present in the real operation room) to assist the apprentices in orienting themselves through the anatomy during gesture.

The realism of the reproduced interaction forces leads to a real immersion feeling while the practitioner is using our simulator. This sensation is reinforced by the quality of the offset visual feedback. For this purpose, the simulator integrates the different mechanical properties of the layers encountered during insertion, in a coherent way between haptic and rendering. Moreover, let us note that the considered gesture is particularly difficult to practice, even for experts. Consequently, they may lose visual contact with the needle, which can be recovered by observing the moving tissues when slightly shivering the tip, although this later not being directly visible in the ultrasound view. The haptic feedback may also be considered by the practitioner to detect whether the bursa is reached or overpassed, as the resistance offered by the underlying tendon is higher than for the fat tissues situated above. Our results show that our implemented methods also provide the user with enough realism for the haptic rendering when the needle pierces the different tissues. This is thanks to the tracking wall algorithm, which renders the cutting forces that allow us to stop the needle during the insertion and to render different tissue stiffness with no chattering problems. Moreover, the implementation of the orientation control allows the user to establish the initial trajectory and offers him the possibility to update it in real-time. Even though this latter is only able to create straight trajectories. Furthermore, the combination of the haptic part with the virtual environment helps to choose the insertion point in the virtual joint, counterbalancing the fixed point of insertion in our mechanical design. To be more realistic, the probe should also offer haptic feedback to users.

Due to its high power/volume ratio, a pneumatic actuator could be inserted inside a volume equivalent to a probe. This actuator could reproduce a haptic feedback to improve the realism of the probe while in contact with the patient. Similar work has been done in [37].

As shown is the Virtual Reality section, some significant scenes have already been designed to cover different stages of the rheumatologist training, from simplified models to a complex shoulder anatomy. One major advantage of our method is the ability to integrate new scenes at a relatively low cost. Indeed, it is sufficient to provide a geometry of the considered layers of tissues, along with their physical properties. The scene can thereby be tuned to handle diversity in morphology,

by altering the geometry of organs, or thickness of the fat layers, for example. In the same manner, many pathological cases could be integrated for the rheumatologist to practice with a great variety of situations, whether they are common or rare. Once the new geometry is set and the organs are labeled, the US view will be computed in real-time to take into account the updated configuration, and the haptic feedback will adjust in the same way to the physical properties of the tissues present in the scene. If applicable, for example for the deltoid, the texture will be synthesized from real images in the right orientation, as long as the corresponding longitudinal and transversal view is available in the texture data bank.

Moreover, a study of the complete training scheme is under progress, that will permitted to identify the progression skills to be acquired by novices, and mandatory requirements of a training simulator at each stage of the learning process. A more complete set of scenes adapted to the progression of the student will be integrated in the framework. In addition, thanks to the flexibility of the mechanical and Virtual Reality parts, the simulator offers the possibly to be adapted to other types of joint like knee, hip, etc. Furthermore, the simulator could be easily adapted to other medical indications with similar gestures, like puncture of tumor tissues, among others.

Finally, the experimental validation of the mechanical part combined with the Virtual Reality rendering, as presented in this paper, was an important preliminary step in the design process of a simulator suitable for training in rheumatology. Everything is now set for the next step: an expanded campaign of measurement combined with a qualitative questionnaire will be carried out with cohorts of novices and experts. This campaign will allow to proceed to content and face validity in order to confirm the relevance of our simulator. Registering trajectories of the tools, and further study them with appropriate settings will help to discriminate novices and experts. That will be a strong marker of the realism and accuracy of the process. In the longer-term, the capacity for the students to transfer the skills acquired on the simulator to the operating room will also be considered, that being the ultimate objective of the simulator design.

ACKNOWLEDGMENT

The authors would like to express their gratitude to the Consejo Nacional de Ciencia y Tecnologia (CONACyT) in Mexico for providing financial support to the PhD student. This work was also supported by the ANR (French National Research Agency) within the IDEFI-SAMSEI (Stratégies d'Apprentissage des Métiers de Santé en Environnement Immersif - ANR-11-IDFI-0034) project.

REFERENCES

[1] J. T. Berger, F. Rosner, and E. J. Cassell, "Ethics of practicing medical procedures on newly dead and nearly dead patients," Journal of General Internal Medicine, vol. 17, no. 10, pp. 774–778, 2002.

[2] R. Brydges, R. Hatala, B. Zendejas, P. Erwin, and D. Cook, "Linking simulation-based educational assessments and patient-related outcomes: A systematic review and meta-analysis," Academic Medicine, vol. 90, pp. 246–256, Feb. 2015. Copyright: Copyright 2017 Elsevier B.V., All rights reserved.

[3] B. Sainsbury, M. Łącki, M. Shahait, M. Goldenberg, A. Baghdadi, L. Cavuoto, J. Ren, M. Green, J. Lee, T. D. Averch, and C. Rossa, "Evaluation of a virtual reality percutaneous nephrolithotomy (pcnl) surgical simulator," Frontiers in Robotics and AI, vol. 6, p. 145, 2020.

[4] N. Herzig, R. Moreau, T. Redarce, F. Abry, and X. Brun, "Nonlinear position and stiffness backstepping controller for a two degrees of freedom pneumatic robot," Control Engineering Practice, vol. 73, pp. 26 – 39, 2018.

[5] T. Sénac, A. Lelevé, R. Moreau, L. Krahenbuhl, F. Sigwalt, and C. Bauer, "Simulating a syringe behavior using a pneumatic cylinder haptic interface," Control Engineering Practice, vol. 90, pp. 231 – 240, 2019.

[6] T. Sénac, A. Lelevé, R. Moreau, L. Krahenbuhl, F. Sigwalt, C. Bauer, and Q. Rouby, "Designing an accurate and customizable epidural anesthesia haptic simulator," IEEE International Conference on Robotics and Automation, pp. 8353–8359, 2019.

[7] N. Herzig, R. Moreau, A. Leleve, and M. T. Pham, "Stiffness control of pneumatic actuators to simulate human tissues behavior on medical haptic simulators," IEEE/ASME International Conference on Advanced Intelligent Mechatronics, AIM, no. July, pp. 1591–1597, 2016.

[8] C. C. J. Alleblas, M. P. H. Vleugels, S. F. P. J. Coppus, and T. E. Nieboer, "The effects of laparoscopic graspers with enhanced haptic feedback on applied forces: a randomized comparison with conventional graspers," Surgical endoscopy, vol. 31, p. 5411—5417, December 2017.

[9] G. Fiard, S.-Y. Selmi, M. Maigron, A. Bellier, E. Promayon, J.-L. Descotes, and J. Troccaz, "Validating the transfer of skills acquired on a prostate biopsy simulator: a prospective, randomized, controlled study," Journal of Surgical Education, vol. 77, no. 4, pp. 953–960, 2020.

[10] C. G. Corrêa, F. L. Nunes, E. Ranzini, R. Nakamura, and R. Tori, "Haptic interaction for needle insertion training in medical applications: The state-of-the-art," Medical Engineering and Physics, vol. 63, pp. 6–25, 2019.

[11] P. V. Balint, D. Kane, J. Hunter, I. B. McInnes, M. Field, and R. D. Sturrock, "Ultrasound guided versus conventional joint and soft tissue fluid aspiration in rheumatology practice: A pilot study," Journal of Rheumatology, vol. 29, no. 10, pp. 2209–2213, 2002.

[12] C. M. Sofka, A. J. Collins, and R. S. Adler, "Use of Ultrasonographic Guidance in Interventional Musculoskeletal," Journal of Ultrasound in Medicine, pp. 21–26, 2001.

[13] L. Barbé, B. Bayle, M. De Mathelin, and A. Gangi, "Needle insertions modelling: Identifiability and limitations," IFAC Proceedings Volumes (IFAC-PapersOnline), vol. 6, no. PART 1, pp. 129–134, 2006.

[14] Y.C. Fung, Biomechanics. Mechanical Properties of Living Tissues. New York: Springer Science ISBN:978-1-4757-2257-4, 2 nd ed., 1993.

[15] H. Kataoka, T. Washio, K. Chinzei, K. Mizuhara, C. Simone, and A. M. Okamura, "Measurement of the Tip and Friction Force Acting on a Needle during Penetration," in Lecture Notes and Computer Science, pp. 216–223, 2002.

[16] Y. Kurita, H. Ohtsuka, K. Nagata, and T. Tsuji, "Haptic rendering of a needle insertion by enhancing the real force response of a base object," in Haptics Symposium 2014, HAPTICS 2014, pp. 357–360, 2014.

[17] C. Forest, O. Comas, C. Vaysière, L. Soler, and J. Marescaux, "Ultrasound and needle insertion simulators built on real patient-based data," Studies in health technology and informatics, vol. 125, pp. 136–139, 2007.

[18] D. Magee, "A computer based simulator for ultrasound guided needle insertion procedures," IEE International Conference on Visual Information Engineering (VIE 2005), pp. 301–308, 2005.

[19] T. R. Coles, N. W. John, D. Gould, and D. G. Caldwell, "Integrating haptics with augmented reality in a femoral palpation and needle insertion training simulation," IEEE Transactions on Haptics, vol. 4, no. 3, pp. 199–209, 2011.

[20] O. Grottke, A. Ntouba, S. Ullrich, W. Liao, E. Fried, A. Prescher, T. M. Deserno, T. Kuhlen, and R. Rossaint, "Virtual reality-based simulator for training in regional anaesthesia," British Journal of Anaesthesia, vol. 103, no. 4, pp. 594–600, 2009.

[21] P.-F. Villard, F. P. Vidal, L. Ap Cenydd, R. Holbrey, S. Pisharody, S. Johnson, A. Bulpitt, N. W. John, F. Bello, and D. A. Gould, "Interventional radiology virtual simulator for liver biopsy," International Journal of Computer Assisted Radiology and Surgery, vol. 9g, pp. 255–267, 2014.

[22] L. Vadcard, "Réflexions à propos de la conception d'environnements de formation par la simulation : le cas de la formation médico-chirurgicale," Raisons Educatives, vol. 21, no. 1, 2017.

[23] N. Abolhassani, R. Patel, and M. Moallem, "Needle insertion into soft tissue: A survey," Medical Engineering and Physics, vol. 29, no. 4, pp. 413–431, 2007.

[24] C. Simone and A. M. Okamura, "Modeling of Needle Insertion Forces for Robot-Assisted Percutaneous Therapy," in Proceedings of the 2002 IEEE International Conference on Robotics & Automation, vol. 2, pp. 2085–2091, May 2002.

[25] M. d. l. A. Alamilla-Daniel, R. Moreau, and R. Tanneguy, "Enhanced tracking wall:A real-time computing method for needle injection on haptic simulators," in IEEE/RSJ International Conference on Intelligent Robots and Systems (IROS), (Las Vegas, United States), , Oct. 2020.

[26] C. Zilles and J. Salisbury, "A constraint-based god-object method for haptic display," in Proceedings IROS 1995, vol. 3, pp. 146–151, 1995.

[27] A. Gordon, A. C. Barnett, I. Kim, and J. Z. Moore, "Needle insertion force model for haptic simulation," ASME 2015 International Manufacturing Science and Engineering Conference, MSEC 2015, vol. 2, pp. 18–20, 2015.

[28] H. R. Malone, O. N. Syed, M. S. Downes, A. L. D'ambrosio, D. O. Quest, and M. G. Kaiser, "Simulation in neurosurgery: A review of computer-based simulation environments and their surgical applications," Neurosurgery, vol. 67, no. 4, pp. 1105–1116, 2010.

[29] A. Asadian, R. V. Patel, and M. R. Kermani, "A distributed model for needle-tissue friction in percutaneous interventions," Proceedings - IEEE International Conference on Robotics and Automation, pp. 1896–1901, 2011.

[30] L. B. Rosenberg, "The use of virtual fixtures as perceptual overlays to enhance operator performance in remote environments.," tech. rep., Defence Technical Information Center, 1992.

[31] K. J. Kuchenbecker, J. Fiene, and G. Niemeyer, "Improving contact realism through event-based haptic feedback," in IEEE Transactions on Visualization and Computer Graphics, vol. 12, pp. 219–229, 2006.

[32] C. Barnouin, F. Zara, and F. Jaillet, "A real-time ultrasound rendering with model-based tissue deformation for needle insertion," in 15th International Conference on Computer Graphics Theory and Applications, GRAPP 2020, (Valleta, Malta), 2020.

[33] T. McReynolds and D. Blythe, Advanced graphics programming using OpenGL. Elsevier, 2005.

[34] D. Panozzo, E. Puppo, and L. Rocca, "Efficient multi-scale curvature and crease estimation," Proceedings of Computer Graphics, Computer Vision and Mathematics (Brno, Czech Rapubic, vol. 1, no. 6, 2010.

[35] D. Gao, Y. Lei, and B. Yao, "Analysis of dynamic tissue deformation during needle insertion into soft tissue," IFAC Proceedings Volumes, vol. 46, no. 5, pp. 684–691, 2013.

[36] J. R. Crouch, C. M. Schneider, J. Wainer, and A. M. Okamura, "A velocity-dependent model for needle insertion in soft tissue," in International Conference on Medical Image Computing and Computer-Assisted Intervention, pp. 624–632, Springer, 2005.

[37] I. Abdallah, F. Gatwaza, N. Morette, A. Lelevé, C. Novales, L. Nouaille, X. Brun, and P. Vieyres, "A Pneumatic Haptic Probe Replica for Tele-Robotized Ultrasonography," in First International Conference on Smart Multimedia (A. Basu and S. Berretti, eds.), vol. 11010 of Lecture Notes in Computer Science, (Toulon, France), pp. 79–89, Springer, Aug. 2018.

Ma Angeles Alamilla Ma. Angeles Alamilla received her BS from the Universidad Politécnica de Pachuca, in Hidalgo, Mexico in 2011, and her Master's degree from the same university in 2014. She worked as a professor in Mechatronics in the Universidad Politécnica de Pachuca from 2014 to 2017. She obtained her Ph.D. degree from Institut National des Sciences Appliquées (INSA) de Lyon, Lyon, France in 2020, focusing on medical robotics and medical simulators.

Charles Barnouin graduated as engineer from Central Lyon in 2016. He obtained his Ph.D degrees in Computer Sciences from Université Lyon 1 (France) in 2020. His research focused on medical simulators and real-time ultrasound rendering.

Richard Moreau received the M.E. in mechanical engineering from Institut National des Sciences Appliquées (INSA) de Lyon, Lyon, France in 2004. The M.S. in biomechanical engineering and Ph.D. in control engineering from the University of Lyon, Lyon, France in 2004 and 2007 respectively. He joined the Laboratoire AMPERE (UMR CNRS 5005), Lyon, France in 2008 as an Assistant Professor. His re search include haptic control in medical robotics area.

Florence Zara is an associate professor since 2005 for computer graphics, animation and virtual reality at LIRIS, Université Lyon1, France. She's defended her Ph.D. in Computer Sciences at Grenoble in 2003. She received her Habilitate Doctor level from the Université de Lyon in 2020. Her research interest is focused on the realization of training simulators for medical gestures. Her expertise includes animation for computer graphics, topological and physical modeling of 3D deformable objects, parallel algorithms, biomechanical simulation of soft tissues, mechanical simulation of pregnant pelvic system, and the coupling of numerical simulations and haptic devices.

Fabrice Jaillet is an associate professor since 1999 at LIRIS Lab, Université Lyon1, France. He graduated as engineer from INSA-Lyon in Computer Science in 1994, and defended his Ph.D. in 1999 in mesh reconstruction from medical imaging for simulating deformable objects. He has been formerly head of the Computer Science department, IUT Lyon1. He also spent three years in Chile, at the CMM in Santiago and DIM in Concepción, and 2 years in Brazil, at LNCC in Petrópolis, on developing new numerical simulation methods. His research includes computational geometry, animation for computer graphics, topological and physically-based modeling of 3D deformable objects, biomechanical simulation of soft tissues, parallel algorithms, augmented reality, haptic devices. He has strong expertise in simulation for medical applications, in particular for computer assisted treatment planning and operation, and training simulators.

Hervé Tanneguy Redarce Hervé Tanneguy Redarce received his PhD in electrical engineering from the Institut National Polytechnique de Grenoble (INPG) in 1984. He received his Habilitate Doctor level from the Institut National des Sciences Appliquées de Lyon (INSA) in 1995. He was assistant professor for 15 years in the Mechanical Engineering Department (INSA de Lyon) and then professor in the Electrical Engineering Department. He teach automatic control and Industrial data processing. In 1999, H. T. Redarce was a visiting researcher at the laboratoire d'Imagerie, de Vision et d'Intelligence Artficielle (LIVIA) de l'Ecole de Technologie Supérieure de l'Université du Québec in Montréal (Canada). Since 2000 he is at the head of the laboratory's robotics research team. His interests include medical robotics, mechatronics systems, and robotic vision. He has published more than 100 papers in various journals and conferences.

Fabienne Coury Fabienne Coury earned her medical degree from Medical School at University of Lyon in 2004, along with specialization in rheumatology. She received a PhD in immunology from Ecole Normale Supérieure in 2008 and completed a postdoctoral fellowship at Harvard Medical School. She is a rheumatology senior physician at Lyon Sud Hospital, Hospices Civils of Lyon and assistant professor at Lyon Sud Medical School. She also developed a training program for medical students using partial tasks trainers at Center for Medical Simulation.